Enhancement of the Lowering Effect on Energy Levels of LUMO by the Formation of B–N Dative Bond for Near-infrared Light Absorption Properties Based on 1,3,4,6,8,9b-Hexaazaphenalene

Hiroyuki Watanabe, Yoshinori Ito, Kazuo Tanaka* and Yoshiki Chujo

Department of Polymer Chemistry, Graduate School of Engineering, Kyoto University

Katsura, Nishikyo-ku, Kyoto 615-8510, Japan

Tel: +81-75-383-2604

Fax: +81-75-383-2605

E-mail: tanaka@poly.synchem.kyoto-u.ac.jp

KEYWORDS

Boron; near infrared; low-lying LUMO; azaphenalene

ABSTRACT

We illustrate the development of 1,3,4,6,8,9b-hexaazaphenalene (6AP) derivatives which exhibit excellent near-infrared (NIR) light absorption properties and deep LUMO levels. The electron-withdrawing character of the 8-nitrogen atom in the 6AP scaffold was enhanced by the introduction of a B-N dative bond. This formation of a boron-nitrogen Lewis acid-base pair succeeded in strengthening the electron-withdrawing ability of the 8-nitrogen atom, which induced the low-lying LUMO levels of the resultant boron complexes. The data from UV–vis–NIR absorption spectroscopy and cyclic voltammetry suggested that these deep LUMO levels were the origins of the narrow HOMO–LUMO gap caused by selectively lowering the LUMO energy level. Furthermore, the enhancement of the molar absorption coefficients was observed in the boron complex compared to other azaphenalene derivatives in the previous reports. From theoretical calculations, the electron-withdrawing character of the 8-nitrogen atom induced the weak but substantial delocalization of the LUMO into the 7,9-positions, where the LUMOs of other azaphenalene derivatives hardly exist. This electronic effect could influence the intrinsic symmetry forbidden character of electronic transition between the HOMO and the LUMO, resulting in the larger molar absorption coefficients by partially transforming to the allow character compared to those of other azaphenalene derivatives. In summary, the introduction of the boron-nitrogen Lewis acid-base pair into the π-conjugated system of azaphenalene afforded the NIR light absorption properties with the ε reaching ~10^4 $M^{-1}cm^{-1}$ and the deep LUMO levels around −4.0 eV (estimated by cyclic voltammetry).

INTRODUCTION

Modulation of energy levels of molecular orbitals is the fundamental technique not only for improving efficiency of organic devices but also for constructing advanced optoelectronic materials. By introducing substituents, we can tune the electronic properties of π-conjugated molecules with some degree. Meanwhile, it has been demonstrated that energy levels of one of the frontier molecular orbitals (FMOs) can be selectively tuned by the modification at the spatially-separated molecular orbitals, called as isolated molecular orbitals, on the basis of azaphenalene derivatives as a scaffold.[1,2] By introducing electron-withdrawing and donating groups at the skeletal carbon where the isolated LUMO and HOMO are distributed, each energy level was specifically lowered, respectively.[2b] As a result, narrow energy gaps can be realized even in the small π-conjugated systems.[2a] Furthermore, we recently found that similar selective tuning of energy levels of FMOs is feasible by the replacement of the skeletal carbon to nitrogen (the aza-substitution) at the isolated FMOs.[3] For example, it was shown that the aza-substitution to the 8-position of hexaazaphenalene (6AP, Figure 1) resulted in the lowered LUMO level and the hardly-affected HOMO level.[3] Then, we were able to obtain light-absorbing materials for long wavelength light without losses of solubility, which is of importance for material usages, because introduction of various functional groups, as well as extension of π-conjugated system, is not necessary.[4]

Figure 1

To realize further bathochromic effects on absorption properties, we presumed the enhancement of electron-accepting ability of the substituted nitrogen. If the electron-

withdrawing nature of the nitrogen atom is enhanced, the LUMO level should be further lowered, leading to narrow HOMO-LUMO gap and subsequently enhancing electron-accepting character of azaphenalene derivatives. When a lone pair which is orthogonal to the π-conjugated system interacts with a Lewis acid, the LUMO level of the compound can be lowered. This phenomenon is generally observed in organic chemistry, as exemplified in the activations of nucleophilic addition reactions to C=O bonds or C≡N bonds.[5] Moreover, this concept of the lowered LUMO level by the Lewis acid-base pair has been applied to the development of *n*-type organic semiconducting materials.[6] The complexation of a boron atom and a nitrogen atom in several π-conjugated scaffolds successfully resulted in the enhanced electron-accepting character of the B←N-containing acenes compared to that of the parent *N*-heteroacenes.

Based on the above speculation, we herein report the selective tuning of the LUMO level of azaphenalene derivatives by the incorporation of a B←N Lewis acid-base pair. The boron atom interacted with the 8-nitrogen atom of 6AP, resulting in the lowered LUMO level (~ −4.0 eV estimated by CV) and the narrow HOMO-LUMO gap (onset wavelength: ~800 nm) of the boron complexes **6a-d**. It was suggested that the 2p orbital of the 8-nitrogen atom, which is a part of the π-conjugated system, was lowered by the introduction of the B←N Lewis acid-base pair. This enhanced electron-withdrawing character of the 8-nitrogen atom resulted in the lowered LUMO level of the boron complex. Furthermore, due to the strongly polarized B–N bond, the π-conjugated system of 6AP was distorted. This distortion relaxed the symmetry-forbidden character of the HOMO–LUMO transition of 6AP, followed by the increased molar absorption coefficients of the 6AP-based boron complexes. This feature was unexpected but should

be a good feature as *n*-type organic semiconductors because large molar absorption coefficients are necessary for non-fullerene acceptors of OPVs and luminescent materials.[7,8]

RESULTS AND DISCUSSION

The introduction of the B←N moiety was achieved via the synthetic route described in Scheme 1. 2,5-Di(*tert*-butyl)-1,3,4,6,8,9b-hexaazaphenalene (6AP, **3**) was synthesized according to the previous report.[3] Compound **3** was successfully brominated by *N*-bromosuccinimide. The brominated 6AP (**4**) was functionalized with 2'-methoxyphenyl groups by the Suzuki–Miyaura cross coupling reaction. Initially, we envisioned that the demethylation of **5a** by boron tribromide[9] should afford a 7,9-(2'-hydroxyphenyl) 6AP **5b**, which was considered to be transformed into the target compounds via the dehydrative condensation reaction between the ligand and boronic acids. However, it was found that, after quenching the reaction by the addition of chloroform (contains < 1 volume % of ethanol as stabilizer) or water, obtained was the boron complex with an ethoxy (**6a**) or a hydroxy group (**6b**) on the boron atom, respectively (Scheme 1). It was presumably because of the high stability of the plausible intermediate **5'** owing to the O^N^O tridentate structure of the ligand. In order to investigate the substituent effects on the boron atom, **5b** was synthesized via another synthetic route (Scheme 2). The ligand was successfully synthesized and reacted with phenylboronic acid or boron trifluoride to afford corresponding boron complexes **6c** or **6d**. The compounds were characterized by ^{1}H and $^{13}C\{^{1}H\}$ NMR and high-resolution mass spectroscopy (HRMS).

Optical properties of the boron complexes were investigated in chloroform (1.0×10^{-5}

M, Figure 2, Table 1). Since significant emission was hardly observed, we focused on absorption properties in this study. Strategic modification successfully afforded the complexes with NIR light-absorption properties. As described in the previous reports, the substituents at the 7,9-positions of azaphenalenes affect the HOMO level.[2a] Correspondingly, **5a** exhibited the red-shifted spectrum compared to that of **3** presumably because the 2-methoxyphenyl groups upraised the HOMO level. Furthermore, the introduction of B←N moiety resulted in the red-shifted spectra of **6a–d** (onset wavelength: ~800 nm). Similar narrow HOMO–LUMO energy gaps were observed in the case of all boron complexes. It is suggested that the combination of the electron-donating groups and the B←N moiety contribute to the narrow HOMO–LUMO energy gap of the boron complexes. It should be noted that their optical properties showed a small dependency on their substituents despite the variety of the substituents on the boron atom.

Figure 2, Table 1

In terms of molar absorption coefficients of the compounds, the unprecedented enhancement was observed by the boron coordination (Table 1). Although it was shown that the aza-substitution is a facile and effective strategy for realizing narrow energy gaps in conjugated systems, we suffer from small magnitude of light-absorption property.[2,3] It is because intrinsic symmetry forbidden character of the transition between FMOs plays a critical role in suppressing probability. Therefore, in the previous studies on azaphenalene derivatives, the molar extinct coefficients of the absorption bands of the S_0–S_1 transition are almost below 10,000 $M^{-1}cm^{-1}$.[2,3] On the other hand, it should be emphasized that the molar absorption coefficients of the boron complexes **6a–d** were as

large as around 10,000 $M^{-1}cm^{-1}$, suggesting that the allowed character of the transition appeared. Leupin and Wirz pointed out that the HOMO–LUMO transition of 9b-azaphenalene should be symmetry-forbidden.[10] Actually, the S_0–S_1 (HOMO-LUMO according to theoretical calculations) transition exhibited small molar absorption coefficient. In the previous reports, we also found that this argument should be applicable to other azaphenalenes including 6AP derivatives.[3] In contrast, from both quantum calculations as listed in Table S1 and experimental data, the light-absorption ability can be boosted by the boron complexation. The enhanced light-absorption properties of the boron complexes implied that the introduction of B←N moiety induced the distortion in the molecular orbital, which may have resulted in the partially allowed character of the HOMO–LUMO transition.

The HOMO and LUMO levels were estimated from quantum calculations (Table S2) and experimentally determined by cyclic voltammetry (CV). The onset potential of first oxidation and reduction peak was converted to the HOMO and LUMO level, respectively, according to the following formula (Table 2)[11]: $E_{HOMO,CV} = -5.10-E_{ox,onset}$ (eV) and $E_{LUMO,CV} = -5.10-E_{red,onset}$ (eV). In Figure 3 the estimated HOMO and LUMO levels are summarized. Since the onset potentials are regarded as useful indices to evaluate the properties of organic electronic materials, we mainly discusses the comparison of the $E_{ox,onset}$s and $E_{red,onset}$s between those of the compounds in this study. The absolute value should be of importance, but the concept of the molecular design would be probed by the relative value of the electrochemical properties.

Figure 3, Table 2

The estimated HOMO and LUMO levels were in accordance with the molecular design. When the pristine 6AP **3** and the 7,9-di(2'-methoxyphenyl) 6AP **5a** were compared, the HOMO level was elevated by the electron-donating substituent, whereas the LUMO level was relatively intact. The introduction the substituents at the 7,9-positions of azaphenalenes affects mainly the HOMO because the HOMO exists at these positions and the LUMO does not. The formation of the B←N moiety by the complexation of the O^N^O tridentate ligand structure and the boron atom successfully resulted in the large shift of the LUMO levels downwards compared to the precursor **5a**. It is suggested that the formation of the boron-nitrogen Lewis acid-base pair successfully induces the enhancement of the electron-withdrawing character of the 8-nitrogen atom in the 6AP scaffold. It should be noted that the effect of the B←N moiety was small on the HOMO level. It is likely that the LUMO exists at the 8-position of 6AP and the HOMO hardly exists, the LUMO should be selectively lowered by this modification. The isolated FMOs, again, should be the origin of these shifts of the FMO energy levels. This is in stark contrast with the case on the introduction of the electronegative moiety to the π-conjugated system, where it resulted in the lowered HOMO *and* LUMO levels.

To elucidate the origin of the obtained properties, theoretical calculations were performed based on density functional theory (DFT) method (B3LYP/6-31+G(d,p) level of theory) using Gaussian 16 C.01 package.[12] The calculated HOMOs and LUMOs are illustrated in Figure 4. In the case of **5a**, the HOMO was delocalized over the substituents at the 7,9-positions, whereas the LUMO was localized on the 6AP scaffold. This type of the extended π-conjugation in either of the FMOs was similarly observed in the case of

other azaphenalene derivatives.[2,3] On the other hand, the FMOs of the boron complexes **6a–d** were different from those of other azaphenalene derivatives in terms of their lobes. The HOMO was similarly delocalized over the substituents, where as a part of the LUMO was delocalized over the oxygen atom and the benzene rings on the 7,9-positions. It is implied that the introduction of the B←N moiety or the formation of the fused structure might be responsible for these distorted LUMOs.

Figure 4

The inductive effects and field effects should be considered in investigating the LUMOs of the boron complexes **6a–d**. We observed the enhancement of the molar absorption coefficient in the case of boron-coordinated 6AP compared to that of 1,3,4,6,9b-pentaazaphenalene (5AP).[3] From the previous results, it can be stated that the strengthened polarity of the chemical bonds between the 7,9-atoms and the 8-atom should induce the increased molar absorption coefficient. When such a local polarity exists at these positions, the LUMO should diffuse into the 7,9-positions, which are positively polarized, to be stabilized. It seems that the formation of B←N moiety upraised the electron-withdrawing properties of the nitrogen atom. As a result, the C(7 or 9)=N8 bonds were more polarized, which was accompanied with the delocalization of the LUMO due to the field effect by the local electric dipole moment at the C=N bonds. The D_{3h} symmetry of the azaphenalene scaffold should be broken by this delocalization of the LUMO. From this discussion, we concluded that the delocalization of the LUMO into the 7,9-positions of 6APs should be the key factor of the improved light-absorption properties.

It is necessary to evaluate the properties of *the atoms in the molecules* in order to prove the hypotheses about the lowered LUMO levels and the larger molar absorption coefficients of the boron complexes **6a–d** compared to those of **5a** or other azaphenalene derivatives. From this point of view, natural bonding orbital (NBO) calculations were performed using NBO 3.1 package incorporated in Gaussian 16 package. In this calculation, the electronic properties of each chemical bond between any pair of the atoms can be obtained. Furthermore, it has been pointed out that each atomic orbital can be more appropriately modeled compared with the result of ordinary *ab initio* calculations.[13] From second-order perturbation theory (SOPT) analyses, it was suggested that the vacant orbital of the boron atom and the lone pair of the 8-nitrogen atom formed a strong Lewis acid-base pair; the strength of the interaction between these two NBOs was estimated to be over 100 kcal/mol, which is comparable to covalent bond.

The Lewis acid-base pair is perpendicular to the π-plane of 6AP and not a component of the π-conjugated system. Therefore, it seemed that atomic orbitals were indirectly influenced by the B←N moiety. Natural atomic orbitals (NAOs) were investigated to clarify the origin of the lower LUMO levels of the boron complexes compared to those of 6AP derivatives and other azaphenalene derivatives in this thesis. In Figure 5, we show schematic diagram of the calculated LUMO levels and the NAO level which corresponds to the $2p_z$ orbital (the component of the π-conjugated system) of the 8-nitrogen atom. The LUMOs were lowered as the NAO of the $2p_z$ orbital of the 8-nitrogen atom was stabilized. The formation of B←N moiety in the boron complexes **6a–d** raised the electron-withdrawing properties of the 8-nitrogen atom, which induced the lowered LUMO level.

Figure 5

The NBO calculation also supported the reason for the enhanced molar absorption coefficients proposed. In the previous study, the aza-substitution at the 8-position distorted the LUMO, which resulted in the larger molar absorption coefficient of boron-coordinated 6AP compared to that of 5AP. The formation of boron-nitrogen Lewis acid-base pair should enhance the electron-withdrawing character of the 8-nitrogen atom, which should lead to the further distorted LUMO level. The intensified electron-withdrawing nature of the 8-nitrogen atoms was also implied in atomic charges of the 7-carbon, 8-nitrogen and 9-carbon atoms calculated by the NBO method (Table 3). The data suggest that the polarization of C(7,9)=N(8) bonds should be large in the other of **3** (both of the carbon atom and the nitrogen atoms are negatively charged) << **5a** (the carbon atoms and the nitrogen atoms are positively and negatively charged, respectively) < **6a-d** (the difference of the charges increased compared to that of **5a**). The diffusion of the LUMO into the 7,9-positions presumably promoted the π-conjugation between the 6AP scaffold and the phenyl ring substituted at those positions. These extensions of the π-conjugated systems are clearly seen in the calculated LUMOs (Figure 4). The spatial separation is an appropriate feature of azaphenalenes to regulate the FMO energy levels independently. However, in terms of the light-absorption properties, symmetry forbidden character in electron transition between the FMOs would be critically unfavorable. It is suggested the distorted FMOs of the boron complexes could contribute to enhancing electron transition probability between FMOs by releasing the forbidden character with some degree.

Table 3

Finally, it should be mentioned that the light-absorption properties of the boron complexes were not influenced by the substituents on the boron atom. From the NBO calculations, it was suggested that the substituents on the boron atom did not strongly affected the NAO which interacted with the 8-nitrogen atom (Figure 5). Furthermore, the NBO charges of **6a-d** were similar as described in Table 3. In this study, the intrinsic Lewis acidity of the boron atom plays a critical role in the optical property changes, such as red-shift of absorption bands and enhancement of light-absorption ability.

CONCLUSION

We demonstrate that the introduction of the B←N moiety to the π-conjugated system of azaphenalenes should be a valid strategy toward narrow HOMO-LUMO gaps, low LUMO levels and improved molar absorption coefficients. From UV–vis–NIR absorption spectra and electrochemical measurements of them, it was suggested that the electron-withdrawing property of the 8-nitrogen atom was enhanced by the interaction between the boron atom, which resulted in the promising properties as *n*-type organic semiconducting materials. The results of the theoretical calculations were consistent with the experimental properties of the boron complexes. Furthermore, the molar absorption coefficients increased unexpectedly compared to those of the ligands. It was suggested that the LUMOs of the boron complex were delocalized into the 7,9-positions of 6AP as a result of the strong electron-withdrawing character of the 8-nitrogen atom in the boron complex. This electronic effect can transform orbital symmetry, followed by enhancement of electronic transition by releasing the symmetry forbidden character. The optical

properties and the electrochemical properties of these boron complexes suggested that the azaphenalene scaffold could be a promising platform to realize tailor-made HOMO–LUMO gap, absolute energy levels of the FMOs and molar absorption coefficient, all of which should be tuned in the development of next-generation organic electronic materials.

ACKNOWLEDGEMENT

This work was partially supported by the Kato Foundation for Promotion of Science (K.T.) and JSPS KAKENHI, grant numbers JP21H02001 and JP21K19002 (for K.T) and JP17J07338 (for H.W.).

REFERENCES

[1] K. Tanaka, Y. Chujo, *Chem. Lett*. **2021**, *50*, 269–279.

[2] a) H. Watanabe, J. Ochi, K. Tanaka, Y. Chujo, *Eur. J. Org. Chem*. **2020**, *2020*, 777–783; b) H. Watanabe, K. Tanaka, Y. Chujo, *Bull. Chem. Soc. Jpn* **2021**, *94*, 1854–1858; c) H. Watanabe, K. Tanaka, Y. Chujo, *J. Org. Chem*. **2019**, *84*, 2768−2778; d) H. Watanabe, Y. Kawano, K. Tanaka, Y. Chujo, *Asian J. Org. Chem*. **2020**, *9*, 259–266; e) H. Watanabe, K. Tanaka, Y. Chujo, *Polymers* **2021**, *13*, 4021; f) H. Watanabe, M. Hirose, K. Tanaka, Y. Chujo, *Chem. Commun*. **2017**, *53*, 5036−5039; g) H. Watanabe, M. Hirose, K. Tanaka, K. Tanaka, Y. Chujo, *Polym. Chem.* **2016**, *7*, 3674−3680; h) H. Yeo, K. Tanaka, M. Hirose, Y. Chujo, *Polym. J*. **2014**, *46*, 688−693.

[3] Watanabe, H.; Tanaka, K.; Chujo, Y. *Asian J. Org. Chem.* **2022**, *11*, e202200221.

[4] a) Narita, A.; Wang, X.-Y.; Feng, X.; Müllen, K. *Chem. Soc. Rev.* **2015**, *44*, 6616–6643; b) Stępień, M.; Gońka, E.; Żyła, M.; Sprutta, N. *Chem. Rev.* **2017**, *117*, 3479–3716; c) Bunz, U. H. F.; Engelhart, J. U.; Lindner, B. D.; Schaffroth, M. *Angew. Chem. Int. Ed.* **2013**, *52*, 3810–3821; d) Bunz, U. H. F. *Acc. Chem. Res.* **2015**, *48*, 1676–1686.

[5] Clayden, J.; Greeves, N.; Warren, S. 2nd ed.; Oxford University Press, 2012.

[6] Min, Y.; Dou, C.; Tian, H.; Geng, Y.; Liu, J.; Wang, L. *Angew. Chem. Int. Ed.* **2018**, *57*, 2000–2004.

[7] a) Cheng, P.; Li, G.; Zhan, X.; Yang, Y. *Nat. Photonics* **2018**, *12*, 131–142; b) Hou, J.; Inganäs, O.; Friend, R. H.; Gao, F. *Nat. Mater.* **2018**, *17*, 119–128; c) Wadsworth, A.; Moser, M.; Marks, A.; Little, M. S.; Gasparini, N.; Brabec, C.

J.; Baran, D.; McCulloch, I. *Chem. Soc. Rev.* **2019**, *48*, 1596–1625.

[8] Aizawa, N.; Pu, Y.-J.; Harabuchi, Y.; Nihonyanagi, A.; Ibuka, R.; Inuzuka, H.; Dhara, B.; Koyama, Y.; Nakayama, K.; Maeda, S.; Araoka, F.; Miyajima, D. *Nature* **2022**, *609*, 502–506.

[9] McOmie, J. F. W.; Watts, M. L.; West, D. E. *Tetrahedron* **1968**, *24*, 2289–2292.

[10] Leupin, W.; Wirz, J. *J. Am. Chem. Soc.* **1980**, *102*, 6068–6075.

[11] Cardona, C. M.; Li, W.; Kaifer, A. E.; Stockdale, D.; Bazan, G. C. *Adv. Mater.* **2011**, *23*, 2367–2371.

[12] Gaussian 16, rev. C.01 Full citation can be found in the Supporting Information.

[13] NBO Version 3.1, Glendening, E. D.; Reed, A. E.; Carpenter, J. E. ; Weinhold, F. For the comparison with molecular orbital theory, see: Weinhold, F. *J. Comp. Chem.* **2012**, *33*, 2363–2379.

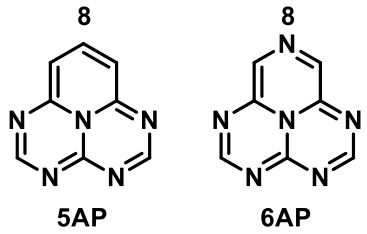

Figure 1. Chemical structures of azaphenales.

Scheme 1. Syntheses of the boron complexes **6a** and **6b**

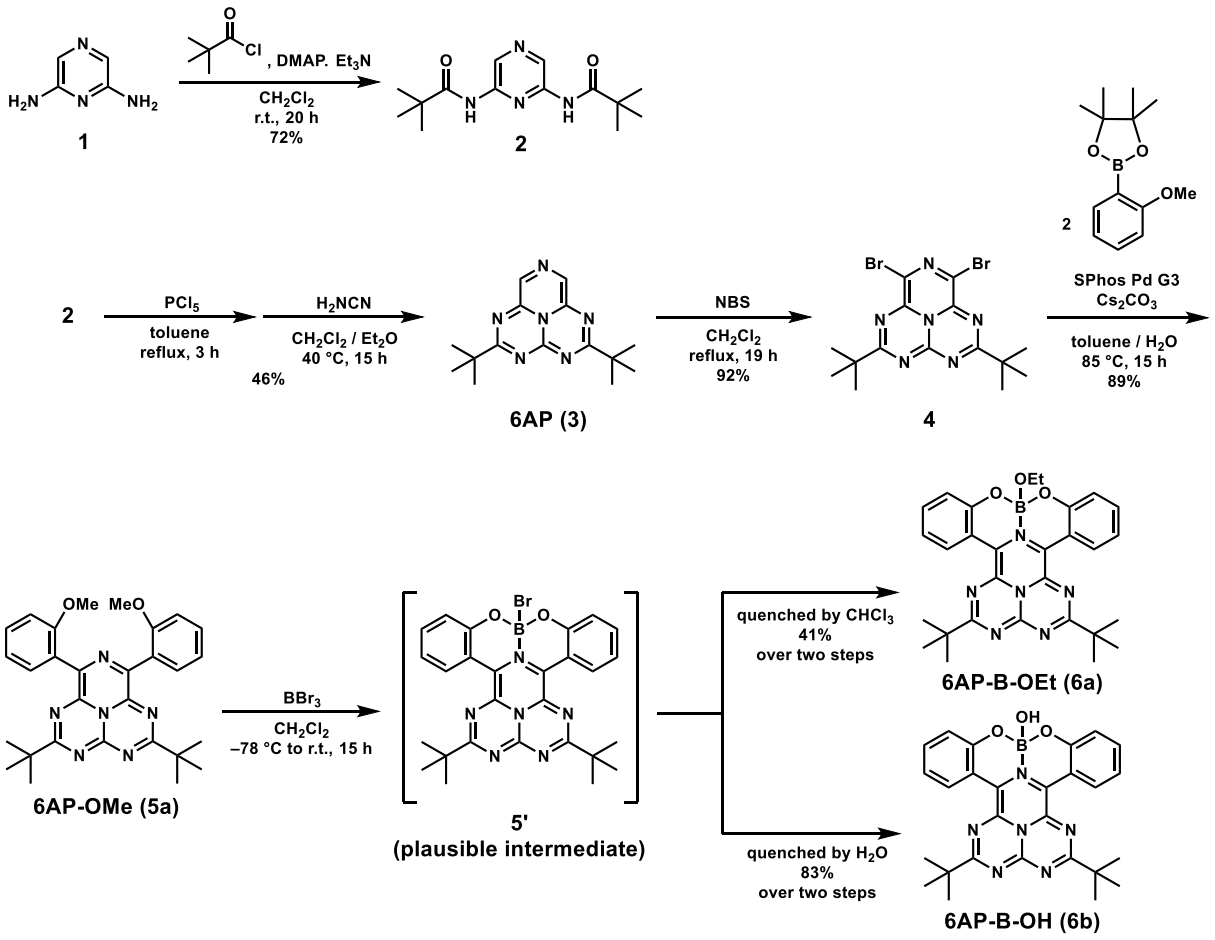

Scheme 2. Syntheses of the boron complexes **6c** and **6d**

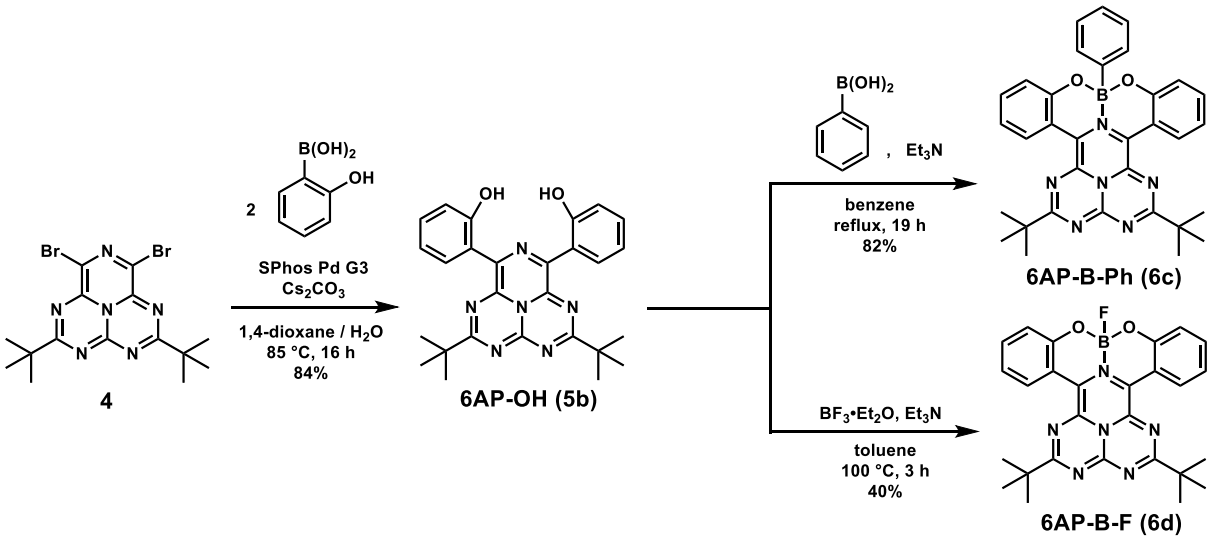

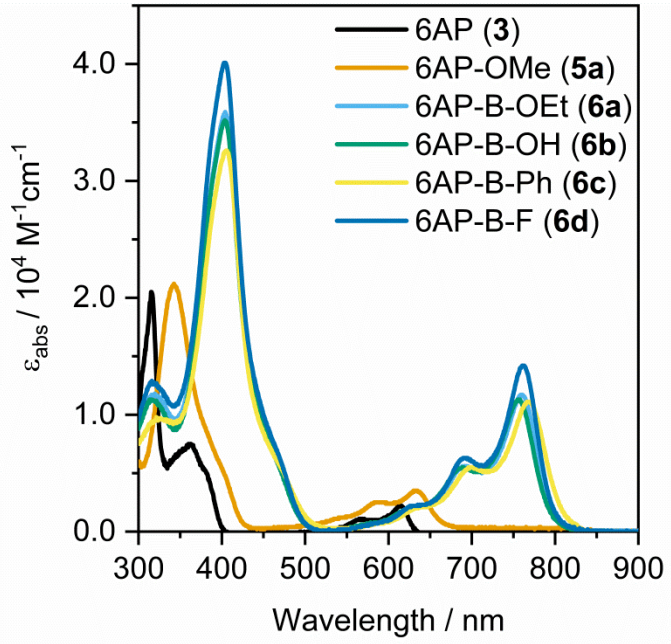

Figure 2. UV–vis–NIR absorption spectra of 6APs **3**, **5a** and **6a–d** (1.0×10^{-5} M in chloroform).

Table 1. Optical properties of **3**, **5a** and **6a–d**[a]

Compound	λ_{abs} / nm	λ_{onset} / nm	ε_{abs} / $M^{-1}\cdot cm^{-1}$
3	611	633	2,100
5a	635	680	3,500
6a	763	821	8,000
6b	761	813	10,900
6c	772	834	11,000
6d	762	821	14,200

[a]Measured in dichloromethane solution (1.0×10^{-5} M).

Table 2. Electrochemical properties of **3**, **5a** and **6a–d**[a]

Compound	$E_{ox,onset}$ / V	$E_{red,onset}$ / V	$E_{HOMO,CV}$[b] / eV	$E_{LUMO,CV}$[c] / eV	E_g[d] / eV
3	0.89	−1.61	−5.99	−3.49	2.50
5a	0.67	−1.75	−5.77	−3.35	2.42
6a	0.67	−1.02	−5.78	−4.08	1.70
6b	0.66	−1.00	−5.76	−4.10	1.66
6c	0.68	−0.98	−5.78	−4.12	1.66
6d	0.71	−0.93	−5.81	−4.17	1.64

[a]Measured in dichloromethane solution (1.0×10^{-3} M) containing 0.1 M tetrabutylammonium hexafluorophosphate (Bu_4NPF_6) as an electrolyte, using a glassy carbon working electrode, a Pt wire counter electrode, an Ag/Ag^+ reference electrode, and a ferrocene/ferrocenium external standard at room temperature with a scan rate of 0.1 Vs^{-1}. [b]$E_{HOMO,CV} = -5.10 - E_{ox,onset}$. [c]$E_{LUMO,CV} = -5.10 - E_{redmonset}$. [d]$E_g = E_{LUMO,CV} - E_{HOMO,CV}$.

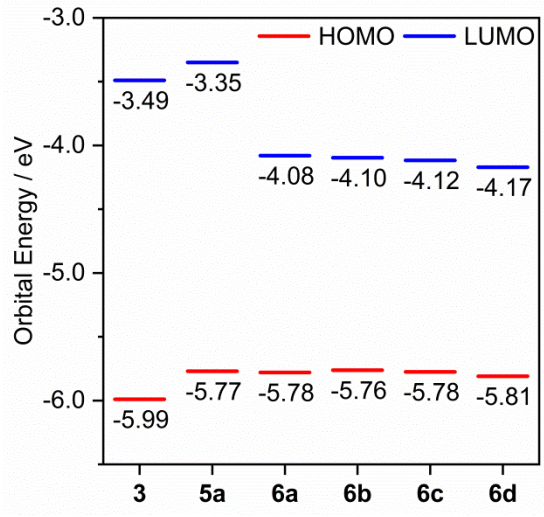

Figure 3. The HOMO and LUMO levels of **3**, **5a** and **6a–d** estimated by CV measurements.

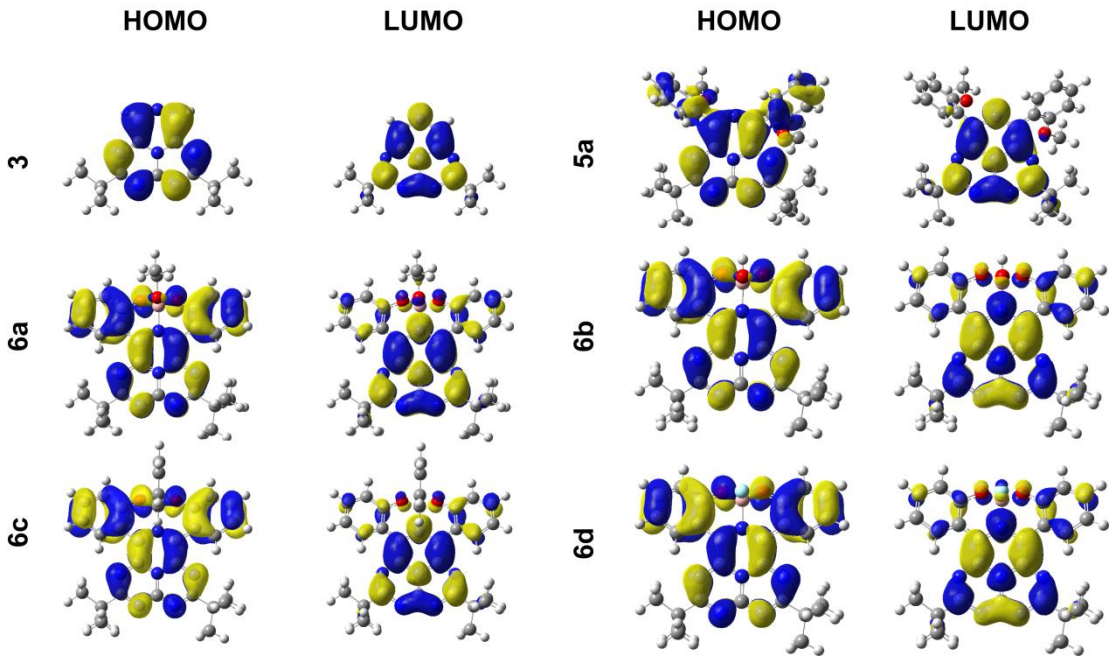

Figure 4. The HOMOs and LUMOs of **3**, **5a** and **6a–d** (B3LYP/6-31+G(d,p) level of theory).

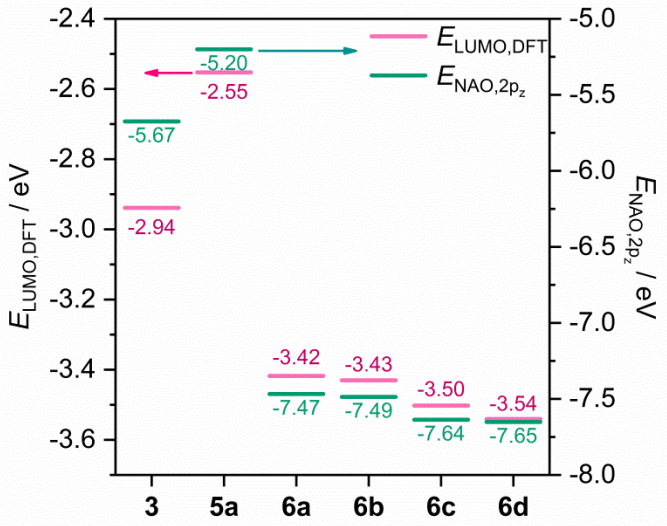

Figure 5. The comparison of the calculated LUMO levels and the calculated NAO $2p_z$ levels of the 8-nitrogen atom. Both values changed in a similar manner.

Table 3. Selected NBO charges of **3**, **5a** and **6a–d**

	NBO charges		
Compound	7-C	8-N	9-C
3	−0.059	−0.375	−0.059
5a	0.147	−0.357	0.137
6a	0.199	−0.450	0.220
6b	0.208	−0.454	0.222
6c	0.211	−0.449	0.220
6d	0.204	−0.466	0.218

GRAPHICAL ABSTRACT

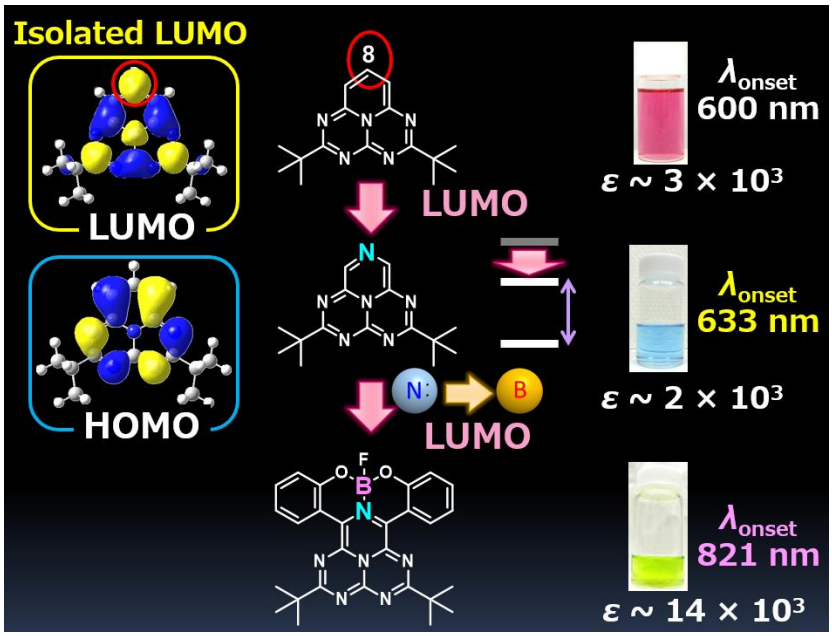

Experimental Section

General

^{1}H (400 MHz), $^{13}C\{^{1}H\}$ (100 MHz), $^{11}B\{^{1}H\}$ (128 MHz) NMR spectra were recorded on JEOL JNM-EX400 or JNM-AL400 spectrometers. ^{1}H NMR spectra were recorded by using tetramethylsilane (TMS) as an internal standard in $CDCl_3$, and by using the residual solvents as internal standard in DMSO-d_6 or $CDCl_2CDCl_2$. $^{13}C\{^{1}H\}$ NMR spectra were recorded by using the residual solvents as internal standard in $CDCl_3$. $^{11}B\{^{1}H\}$ NMR spectra were recorded by using $BF_3{\cdot}Et_2O$ as an external standard. High-resolution mass spectra (HRMS) were obtained on a Thermo Fisher EXACTIVE Plus for electron spray ionization (ESI) or atmospheric pressure chemical ionization (APCI). UV–vis absorption spectra were recorded on a Shimadzu UV-3600 spectrophotometer. Cyclic voltammetry (CV) was carried out on a BAS ALS-Electrochemical-Analyzer Model 600D with a glassy carbon working electrode, a Pt counter electrode, an Ag/Ag^{+} reference electrode, and the ferrocene/ferrocenium external reference at a scan rate of 0.1 Vs^{-1}. All reactions were performed under argon atmosphere.

Theoretical Calculation

Density functional theory (DFT) calculations were performed using Gaussian 16 C.01 package.[1] B3LYP functional and 6-31+G(d,p) basis set were used in all calculations. After the optimization calculations, we performed the frequency calculations to confirm the optimized structure. No imaginary frequencies were found. Kohn-Sham orbitals of 5APs were generated from these optimized structures using GaussView 6 (isovalue: 0.02, Figure 4 in the main text).

Natural Bonding Orbital (NBO) calculations were performed using NBO 3.1 package

incorporated with the Gaussian package. The saveNBOs options were used in order to obtain the decomposition of the NBOs to the NAOs.

Materials

2,5-Di(*tert*-butyl)-1,3,4,6,8,9b-hexaazaphenalene was synthesized according to the procedure described in the previous report.[2] Reagents (*N*-bromosuccinimide, (2-dicyclohexylphosphino-2',6'-dimethoxybiphenyl)(2-(2'-amino-1,1'-biphenyl))palladium(II) methanesulfonate (SPhos Pd G3), 2-methoxyphenylboronic acid pinacol ester, 2-hydroxyphenylboronic acid, phenylboronic acid, cesium carbonate, boron tribromide dichloromethane solution (ca. 1 M), boron trifluoride diethyl etherate ($BF_3 \cdot Et_2O$)) and solvents (dichloromethane, toluene, 1,4-dioxane and benzene) were purchased from commercial sources and used without further purification. Diethyl ether (Et_2O) and triethylamine (NEt_3) were purified using a two-column solid-state purification system (Glasscontour System, Joerg Meyer, Irvine, CA). Water for the Suzuki–Miyaura cross coupling reactions was degassed by Ar bubbling before use.

Synthetic Procedures

• Synthesis of 7,9-dibromo-1,3,4,6,8,9b-hexaazaphenalene (**4**)

A CH_2Cl_2 (100 mL) solution of **3** (0.570 g, 2.00 mmol) and *N*-bromosuccinimide (0.750 g, 4.20 mmol) was refluxed for 19 h. The solution was washed by H_2O (3 × 100 mL) and brine (1 × 100 mL). The organic layer was dried over $MgSO_4$. After filtration, the solvent was removed by a rotary evaporator. The residue was purified by column chromatography on silica gel (eluent: hexane / CH_2Cl_2 = 1:1 (v/v), R_f = 0.41) and then the solvents were evaporated to afford **4** as a blue solid (0.81 g, 1.8 mmol, 92% isolated

yield). ^{1}H NMR ($CDCl_3$, ppm): δ 1.22 (s), $^{13}C\{^{1}H\}$ NMR ($CDCl_3$, ppm): δ 190.5, 160.5, 145.4, 120.2, 40.3, 27.7. HRMS (APCI-orbitrap) *m*/*z*: $[M+H]^+$ Calcd. for $C_{15}H_{18}Br_2N_6$+H 441.0032; Found 441.0032.

• Synthesis of 7,9-di(2'-methoxyphenyl)-1,3,4,6,8,9b-hexaazaphenalene (6AP-OMe, **5a**)

To a toluene (2 mL) solution of **4** (0.133 g, 0.300 mmol), 2-methoxyphenylboronic acid pinacol ester (0.147 g, 0.630 mmol), SPhos Pd G3 (0.0260 g, 0.0300 mmol) and Cs_2CO_3 (0.977 g, 3.00 mmol) was added degassed water (2 mL). The mixture was stirred at 85 °C for 15 h. The reaction mixture was allowed to cool to room temperature and diluted by $CHCl_3$ (20 mL). The organic layer was washed by H_2O (3 × 40 mL) and brine (1 × 20 mL), and then dried over $MgSO_4$. After filtration, the solvents were removed by a rotary evaporator. The residue was purified by column chromatography on silica gel (eluent: CH_2Cl_2, R_f = 0.42) and then the solvent was evaporated to afford **5a** as a blue solid (0.13 g, 0.27 mmol, 89% isolated yield). ^{1}H NMR ($CDCl_3$, ppm): δ 7.34 (d, J = 7.6 Hz, 4H), 6.96 (td, J = 7.6, 0.8 Hz, 2H), 6.89 (d, J = 8.0 Hz, 2H), 3.84 (s, 6H), 1.09 (s, 18H). $^{13}C\{^{1}H\}$ NMR ($CDCl_3$, ppm): δ 187.6, 161.0, 157.4, 144.1, 139.6, 130.7, 130.1, 125,0, 120.4, 110.4, 55.3, 39.5, 27.1. HRMS (ESI-orbitrap) *m*/*z*: $[M+Na]^+$ Calcd. for $C_{29}H_{32}N_6O_2$+Na 519.2479; Found 519.2474.

• Synthesis of 7,9-di(2'-hydroxyphenyl)-1,3,4,6,8,9b-hexaazaphenalene (6AP-OH, **5b**)

To a 1,4-dioxane (9 mL) solution of **4** (0.133 g, 0.300 mmol), 2-hydroxyphenylboronic acid (0.0869 g, 0.630 mmol), SPhos Pd G3 (0.0260 g, 0.0300 mmol) and Cs_2CO_3 (0.489 g, 1.50 mmol) was added degassed water (1 mL). The mixture was stirred at 85 °C for 16 h. The reaction mixture was allowed to cool to room temperature and diluted by $CHCl_3$

(10 mL). The organic layer was washed by H_2O (3 × 30 mL) and brine (1 × 20 mL), and then dried over Na_2SO_4. After filtration, the solvents were removed by a rotary evaporator. The residue was purified by column chromatography on silica gel (eluent: CH_2Cl_2 / hexane = 10:1 (v/v), R_f = 0.42) and then the solvents were evaporated to afford **5b** as a blue solid (0.12 g, 0.25 mmol, 84% isolated yield). ^{1}H NMR ($CDCl_3$, ppm): δ 9.98 (s, 2H), 8.02 (dd, J = 8.1, 1.6 Hz, 2H), 7.38–7.33 (m, 2H), 7.02–6.95 (m, 4H), 1.27 (s, 18H). ^{13}C{^{1}H} NMR ($CDCl_3$, ppm): δ 188.9, 160.7, 157.1, 142.4, 138.3, 131.8, 129.8, 120.6, 120.0, 119.2, 40.2, 27.9. HRMS (APCI-orbitrap) *m*/*z*: $[M+Na]^+$ Calcd. for $C_{27}H_{28}N_6O_2$+Na 491.2166; Found 491.2171.

• Synthesis of 6AP-B-OEt (**6a**)

A CH_2Cl_2 (1 mL) solution of **5a** (9.93 mg, 0.0200 mmol) was stirred and subsequently cooled to –78 °C. To the solution was added slowly boron tribromide dichloromethane solution (1 M) (0.400 mL, 0.100 g, 0.400 mmol) dropwise. After stirred at –78 °C for 1 h, the reaction mixture was carried out at room temperature for 13 h. The reaction mixture was diluted by $CHCl_3$ (10 mL, contained EtOH 0.3~1.0 % as stabilizer). The organic layer was washed by saturated $NaHCO_3$ aq. (3 × 20 mL), H_2O (1 × 20 mL) and brine (1 × 20 mL). The organic layer was dried over $MgSO_4$. After filtration, the solvents were removed by a rotary evaporator. The residue was purified by column chromatography on silica gel (eluent: CH_2Cl_2 / MeOH = 40:1 (v/v), R_f = 0.58) and then the solvents were evaporated to afford **6a** as a green solid (4.3 mg, 0.0082 mmol, 41% isolated yield). ^{1}H NMR ($CDCl_3$, ppm): δ 8.56 (dd, J = 8.3, 1.4 Hz, 2H), 7.38 (ddd, J = 8.3, 7.1, 1.4 Hz, 2H), 7.07 (dd, J = 8.1, 1.0 Hz, 2H), 6.94–6.90 (m, 2H), 3.48 (q, J = 7.0 Hz, 2H), 1.27 (s, 18H), 0.83 (t, J = 7.0 Hz, 3H). ^{13}C{^{1}H} NMR ($CDCl_3$, ppm): δ 188.7, 160.8, 156.0, 146.4, 133.3, 129.7,

129.3, 119.4, 119.1, 116.8, 56.5, 40.4, 27.9, 17.6. $^{11}B\{^{1}H\}$ NMR ($CDCl_3$, ppm): δ 2.55. HRMS (APCI-orbitrap) *m*/*z*: $[M+H]^+$ Calcd. for $C_{29}H_{31}BN_6O_3$+H 523.2623; Found 523.2624.

• Synthesis of 6AP-B-OH (**6b**)

A CH_2Cl_2 (1 mL) solution of **5a** (9.93 mg, 0.0200 mmol) was stirred and subsequently cooled to –78 °C. To the solution was added slowly boron tribromide dichloromethane solution (1 M) (0.400 mL, 0.100 g, 0.400 mmol) dropwise. After stirred at –78 °C for 1 h, the reaction mixture was carried out at room temperature for 18 h. The reaction mixture was diluted by CH_2Cl_2 (10 mL) and was carefully added to H_2O at 0 °C for quenching the reaction. The organic layer was washed by saturated $NaHCO_3$ aq. (3 × 15 mL), H_2O (1 × 15 mL) and brine (1 × 15 mL), and then dried over Na_2SO_4. After filtration, the solvent was removed by a rotary evaporator. The residue was purified by column chromatography on silica gel (eluent: $CHCl_3$ / MeOH = 40:1 (v/v), R_f = 0.34) and then the solvents were evaporated to afford **6b** as a green solid (8.2 mg, 0.017 mmol, 83% isolated yield). ^{1}H NMR (DMSO-d_6, ppm): *δ* 8.59–8.57 (m, 2H), 7.36–7.32 (m, 2H), 6.91 (t, *J* = 6.9 Hz, 4H), 4.39 (s, 1H), 1.21 (s, 18H).$^{13}C\{^{1}H\}$ NMR ($CDCl_3$, ppm): δ 189.0, 160.9, 155.8, 146.5, 133.6, 129.6, 129.5, 119.8, 119.5, 116.6, 40.6, 28.1. $^{11}B\{^{1}H\}$ NMR ($CDCl_3$, ppm): δ 1.96. HRMS (ESI-orbitrap) *m*/*z*: $[M+Na]^+$ Calcd. for $C_{27}H_{27}BN_6O_3$+Na 517.2130; Found 517.2129.

• Synthesis of 6AP-B-Ph (**6c**)

A Schlenk flask was used after dehydrated by a heat gun. A mixture of **5b** (9.37 mg, 0.0200 mmol), phenylboronic acid (2.68 mg, 0.0220 mmol), Et_3N (0.0100 mL, 7.26 mg,

0.0717 mmol) and benzene (0.5 mL) was placed in the Schlenk flask, and then refluxed for 19 h. The solvent was dried, and the green crude solid was dissolved in $CHCl_3$ (10 mL). The solution was washed by H_2O (3 × 15 mL) and brine (1 × 15 mL). The organic layer was dried over Na_2SO_4. After filtration, the solvent was removed by a rotary evaporator. The residue was purified by column chromatography on silica gel (eluent: CH_2Cl_2 / hexane = 4:1 (v/v), R_f = 0.27) and then the solvents were evaporated to afford **6c** as a green solid (9.1 mg, 0.016 mmol, 82% isolated yield). ^{1}H NMR (400 MHz; $CDCl_3$): δ 8.42 (dd, J = 8.1, 1.4 Hz, 2H), 7.32–7.28 (m, 2H), 7.23–7.21 (m, 2H), 7.06 (m, 3H), 6.97 (dd, J = 8.1, 0.7 Hz, 2H), 6.87–6.83 (m, 2H), 1.28 (s, 18H). ^{13}C{^{1}H} NMR ($CDCl_3$, ppm): δ 188.9, 160.8, 156.3, 146.4, 133.6, 131.4, 130.1, 129.1, 127.4, 127.1, 119.7, 118.9, 117.2, 40.5, 27.9. ^{11}B{^{1}H} NMR ($CDCl_3$, ppm): δ 5.69. HRMS (ESI-orbitrap) m/z: $[M+Na]^+$ Calcd. for $C_{33}H_{31}BN_6O_2$+Na 577.2494; Found 577.2500.

• Synthesis of 6AP-B-F (**6d**)

To a toluene (2 mL) solution of **5b** (0.0469 g, 0.100 mmol) was added BF_3•Et_2O (0.126 mL, 0.142 g, 1.00 mmol) and Et_3N (0.139mL, 0.101 g, 1.00 mmol). The mixture was stirred at 100 °C for 3 h. The reaction mixture was cooled to room temperature, and the reaction was quenched by the addition of EtOH (1 mL). The solution was diluted by toluene (10 mL) and the solvents were removed by a rotary evaporator. The residue was purified by column chromatography on silica gel (eluent: CH_2Cl_2), R_f = 0.51) and then the solvent was evaporated to afford **6d** as a green solid (0.020 g, 0.040 mmol, 40 % isolated yield). ^{1}H NMR ($CDCl_3$, ppm): δ 8.58 (d, J = 8.3 Hz, 2H), 7.40 (dd, J = 8.3, 7.1 Hz, 2H), 7.11 (d, J = 8.3 Hz, 2H), 6.95 (m, 2H), 1.28 (s, 18H). ^{13}C{^{1}H} NMR ($CDCl_3$, ppm): δ 189.1, 160.7, 154.9, 146.6, 133.7, 129.5, 129.1, 119.8, 119.6, 116.0, 40.5, 27.9.

$^{11}B\{^{1}H\}$ NMR ($CDCl_3$, ppm): δ 5.69. HRMS (ESI-orbitrap) *m*/*z*: $[M+Na]^+$ Calcd. for $C_{27}H_{26}BFN_6O_2$+Na 519.2087; Found 519.2085.

Results of DFT calculations

Table S1. Calculated electronic transitions

compound	λ_{max} / nm	f[a]	Component (coefficient)
3	537	0.0146	HOMO => LUMO (0.69) HOMO => LUMO+1 (–0.13)
	330	0.1463	HOMO => LUMO+1 (0.67)
	290	0.2346	HOMO => LUMO+2 (0.69)
5a	560	0.0405	HOMO => LUMO (0.69) HOMO => LUMO+1 (0.13)
	350	0.1054	HOMO => LUMO+1 (0.56)
	331	0.3509	HOMO => LUMO+2 (0.68)
6a	744	0.0793	HOMO => LUMO (0.69) HOMO => LUMO+1 (0.12)
	442	0.1187	HOMO => LUMO+1 (0.66)
	400	0.2656	HOMO => LUMO+2 (0.62)
6b	745	0.0828	HOMO => LUMO (0.69) HOMO => LUMO+1 (0.12)
	442	0.1193	HOMO => LUMO+1 (0.66)
	400	0.2581	HOMO => LUMO+2 (0.62)
	382	0.1846	HOMO-3 => LUMO (0.57) HOMO => LUMO+2 (-0.30)
6c	762	0.0745	HOMO => LUMO (0.69) HOMO => LUMO+1 (–0.11)
	446	0.1045	HOMO => LUMO+1 (0.66)
	405	0.2065	HOMO => LUMO+2 (0.59)
	392	0.1686	HOMO-5 => LUMO (0.54) HOMO => LUMO+2 (0.35)
6d	739	0.0865	HOMO => LUMO (0.69) HOMO => LUMO+1 (0.13)
	439	0.1247	HOMO => LUMO+1 (0.66)
	399	0.2157	HOMO => LUMO+2 (0.59)
	382	0.2239	HOMO-3 => LUMO (0.54) HOMO => LUMO+2 (0.35)

[a] Oscillator strength.

Table S2. Calculated frontier orbital energies

	E_{HOMO} / eV	E_{LUMO} / eV
3	-6.13	–2.94
5a	–5.58	–2.55
6a	–5.65	–3.42
6b	–5.65	–3.43
6c	–5.69	–3.50
6d	–5.77	–3.54

REFERENCES

1. Gaussian 16, Revision B.01, Frisch, M. J.; Trucks, G. W.; Schlegel, H. B.; Scuseria, G. E.; Robb, M. A.; Cheeseman, J. R.; Scalmani, G.; Barone, V.; Petersson, G. A.; Nakatsuji, H.; Li, X.; Caricato, M.; Marenich, A. V.; Bloino, J.; Janesko, B. G.; Gomperts, R.; Mennucci, B.; Hratchian, H. P.; Ortiz, J. V.; Izmaylov, A. F.; Sonnenberg, J. L.; Williams-Young, D.; Ding, F.; Lipparini, F.; Egidi, F.; Goings, J.; Peng, B.; Petrone, A.; Henderson, T.; Ranasinghe, D.; Zakrzewski, V. G.; Gao, J.; Rega, N.; Zheng, G.; Liang, W.; Hada, M.; Ehara, M.; Toyota, K.; Fukuda, R.; Hasegawa, J.; Ishida, M.; Nakajima, T.; Honda, Y.; Kitao, O.; Nakai, H.; Vreven, T.; Throssell, K.; Montgomery, J. A., Jr.; Peralta, J. E.; Ogliaro, F.; Bearpark, M. J.; Heyd, J. J.; Brothers, E. N.; Kudin, K. N.; Staroverov, V. N.; Keith, T. A.; Kobayashi, R.; Normand, J.; Raghavachari, K.; Rendell, A. P.; Burant, J. C.; Iyengar, S. S.; Tomasi, J.; Cossi, M.; Millam, J. M.; Klene, M.; Adamo, C.; Cammi, R.; Ochterski, J. W.; Martin, R. L.; Morokuma, K.; Farkas, O.; Foresman, J. B.; Fox, D. J. Gaussian, Inc., Wallingford CT, 2016.
2. Watanabe, H.; Tanaka, K.; Chujo, Y. *Asian J. Org. Chem.* **2022**, *11*, e202200221.

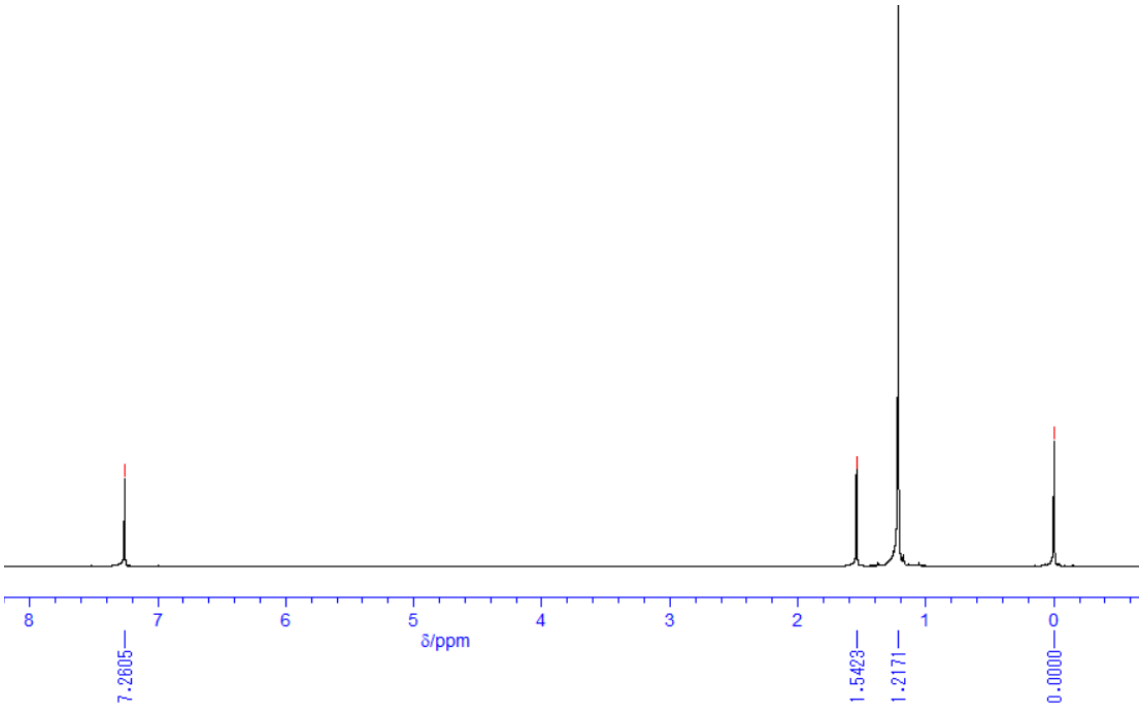

Chart 1. ^{1}H NMR spectrum of **4**.

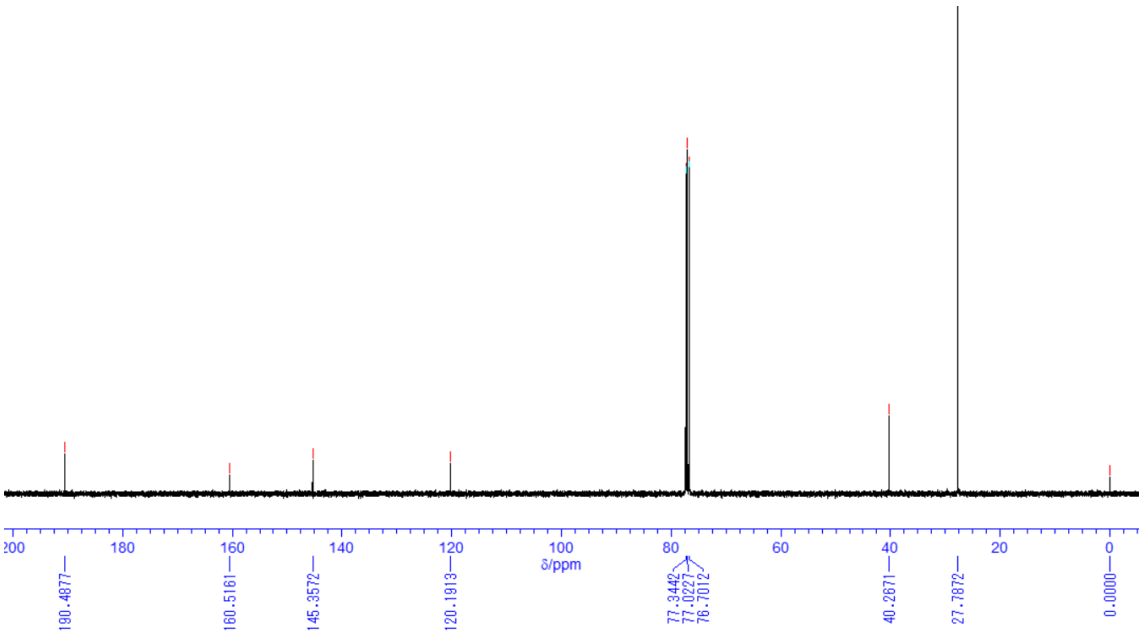

Chart 2. ^{13}C NMR spectrum of **4**.

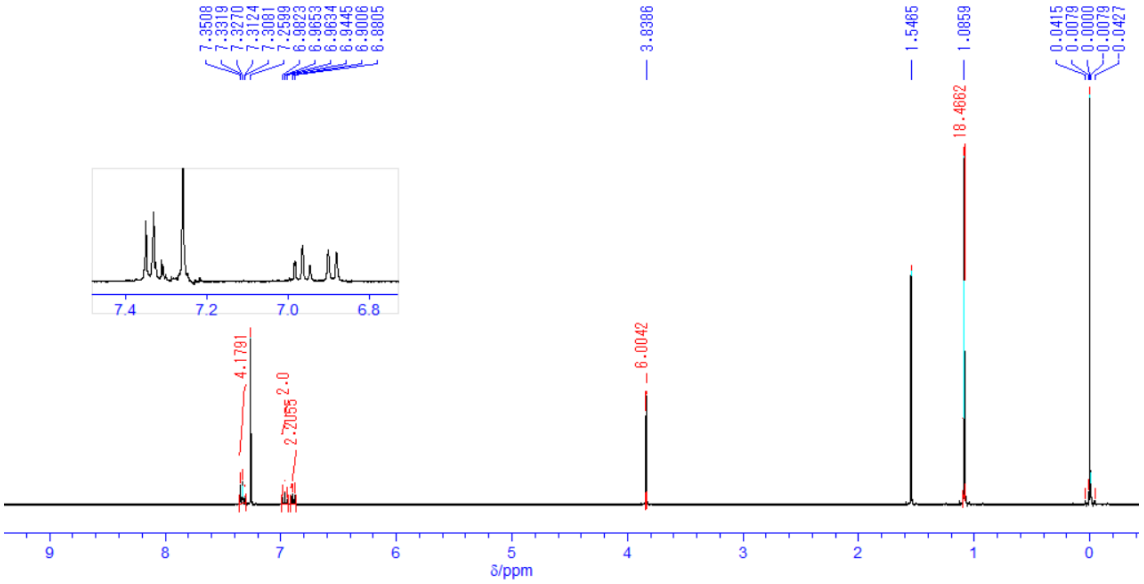

Chart 3. ^{1}H NMR spectrum of **5a**.

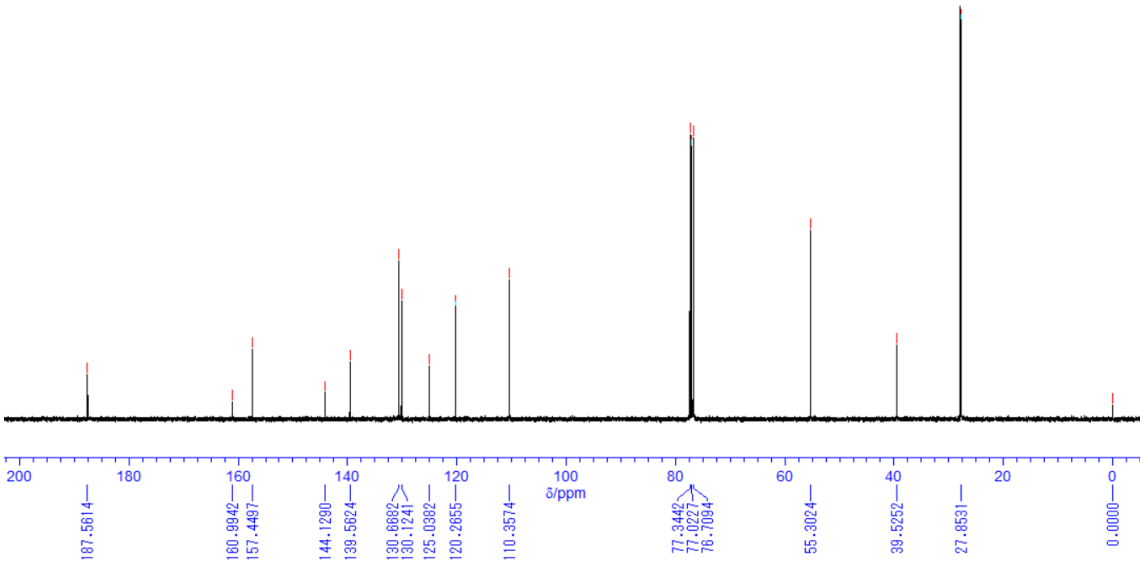

Chart 4. ^{13}C NMR spectrum of **5a**.

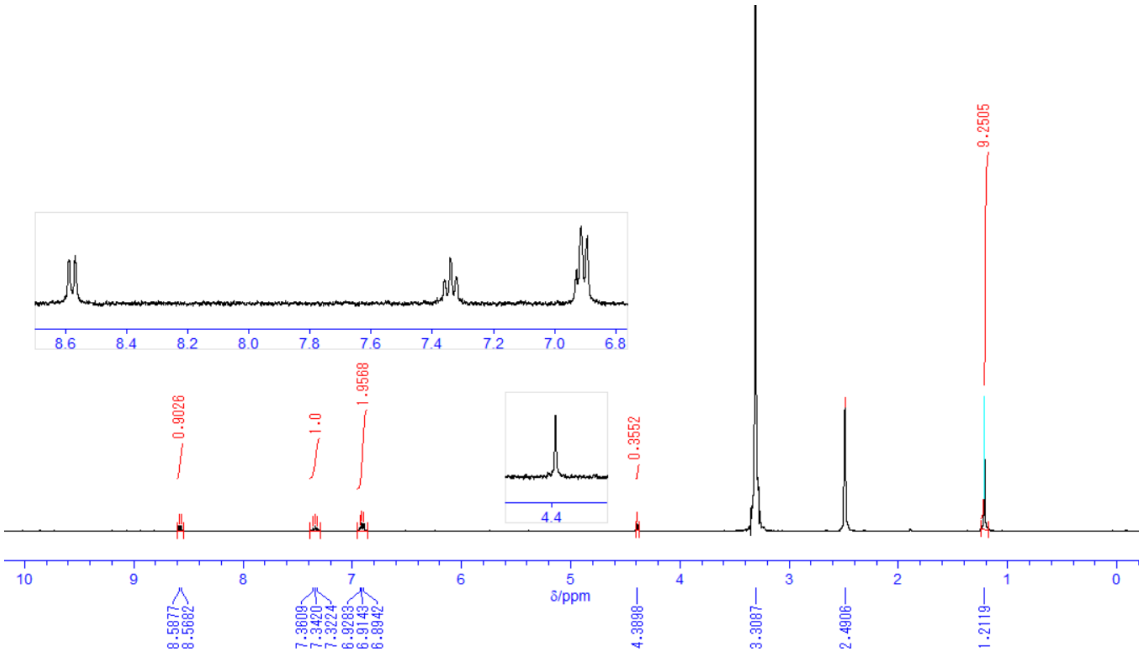

Chart 5. ^{1}H NMR spectrum of **5b**.

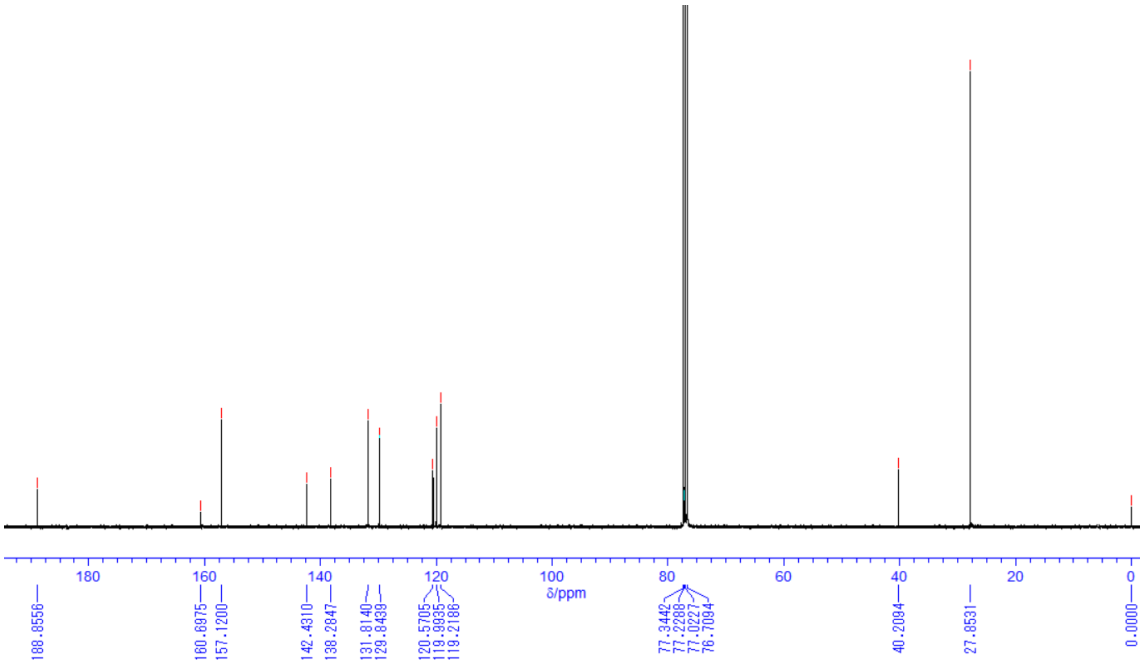

Chart 6. ^{13}C NMR spectrum of **5b**.

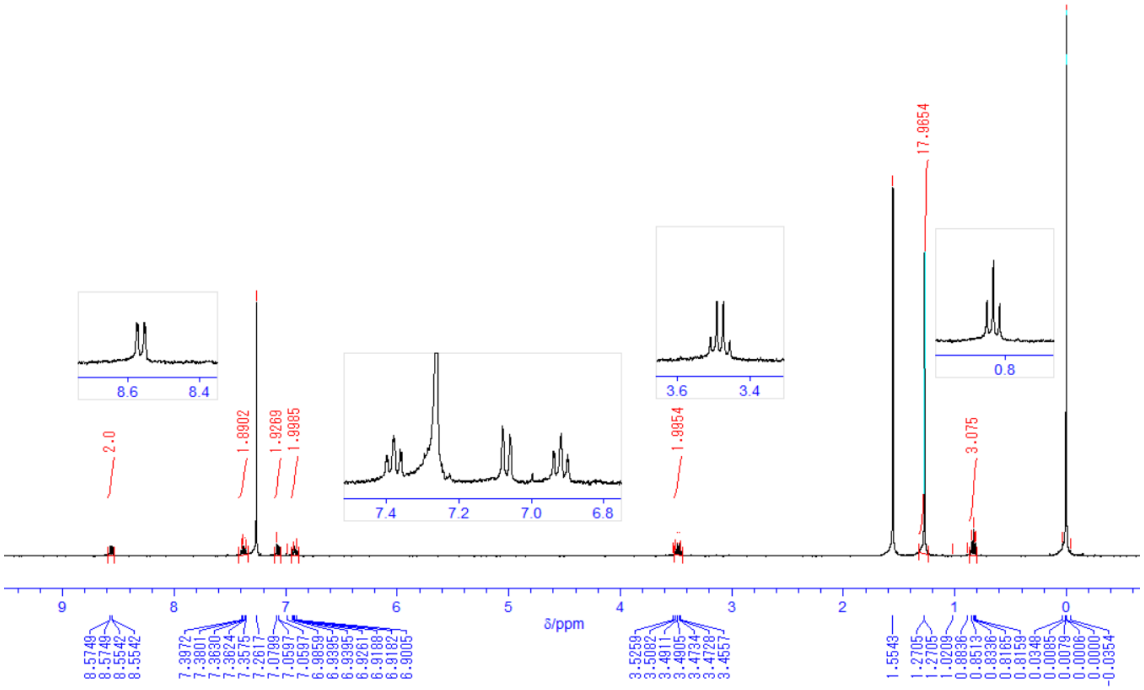

Chart 7. ^{1}H NMR spectrum of **6a**.

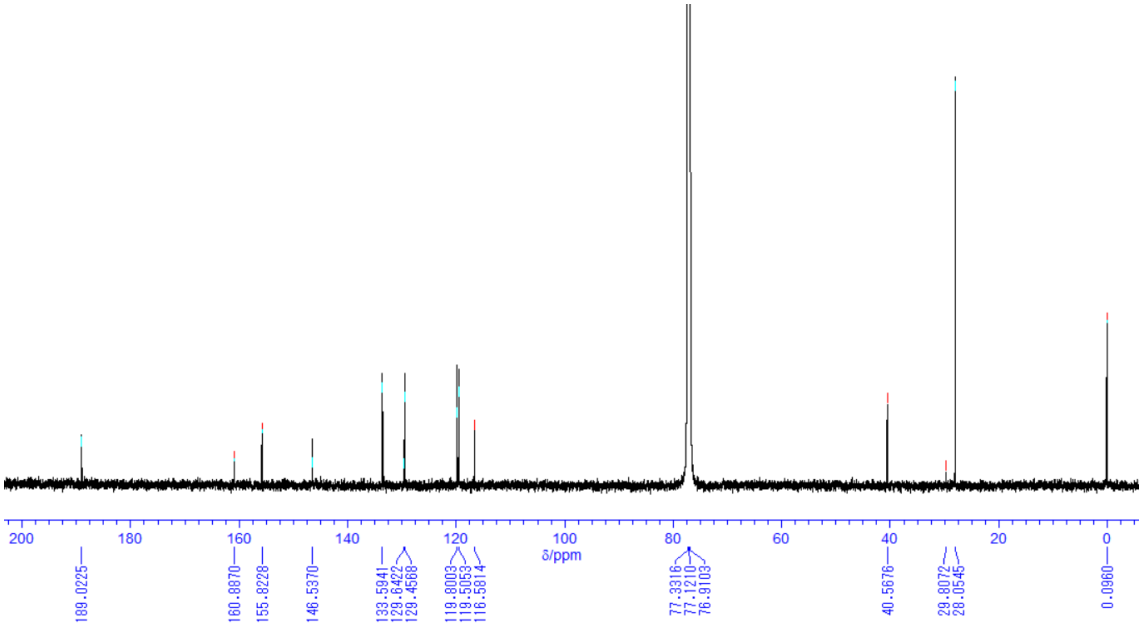

Chart 8. ^{13}C NMR spectrum of **6a**.

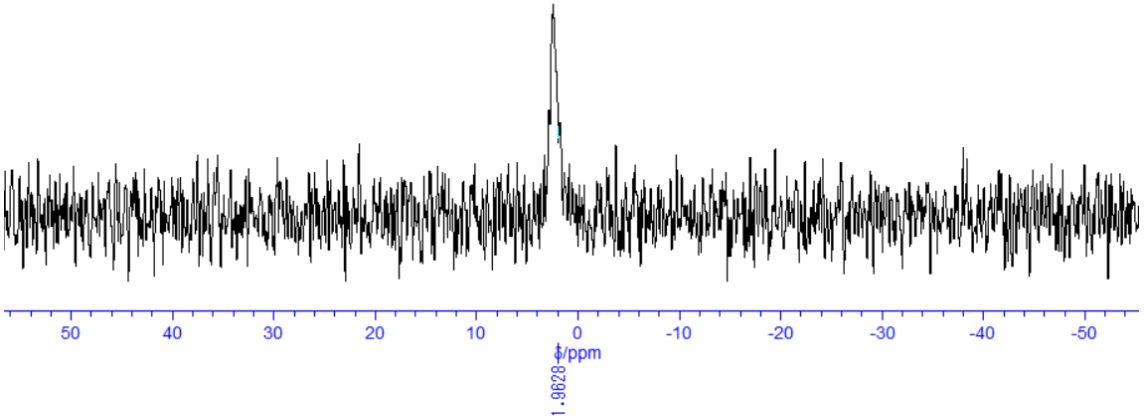

Chart 9. ^{11}B NMR spectrum of **6a**.

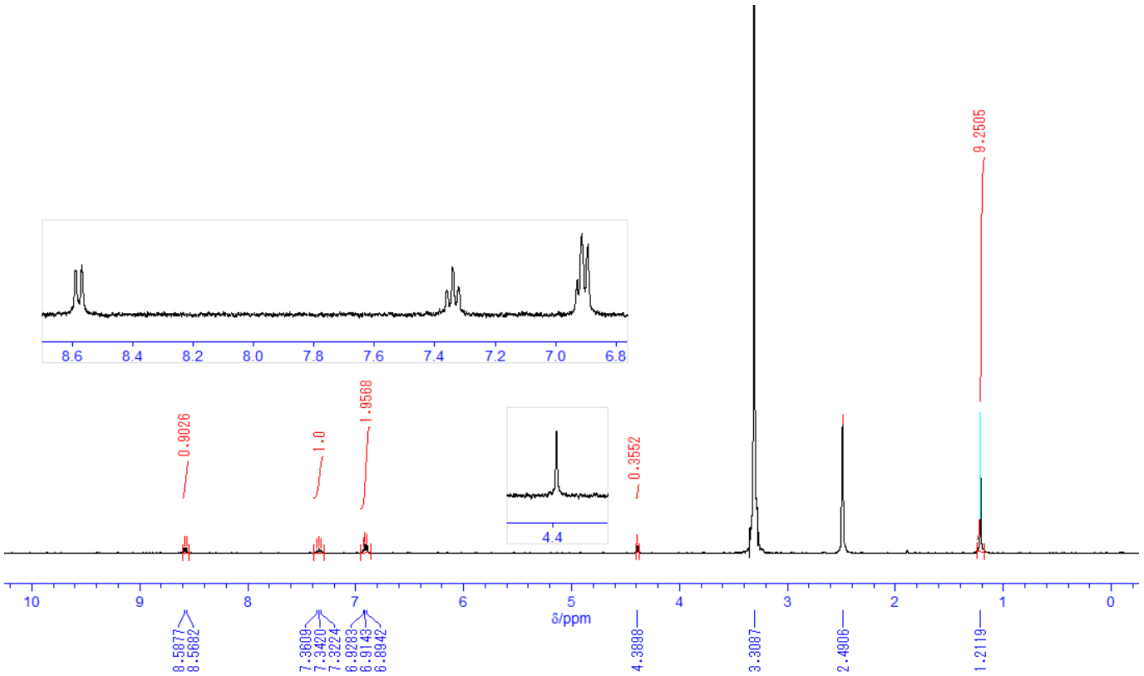

Chart 10. ^{1}H NMR spectrum of **6b**.

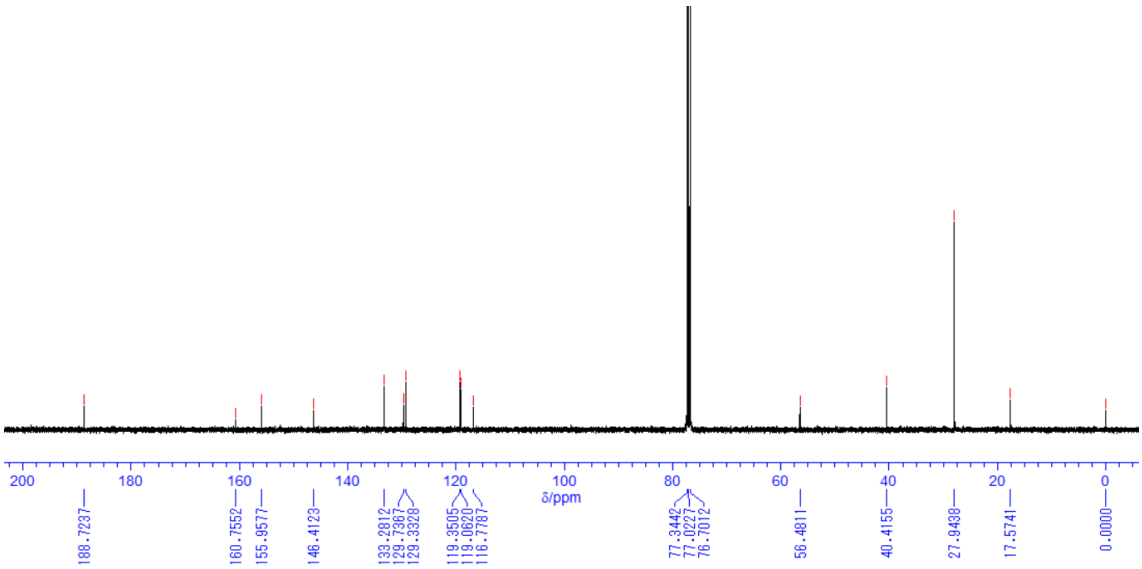

Chart 11. ^{13}C NMR spectrum of **6b**.

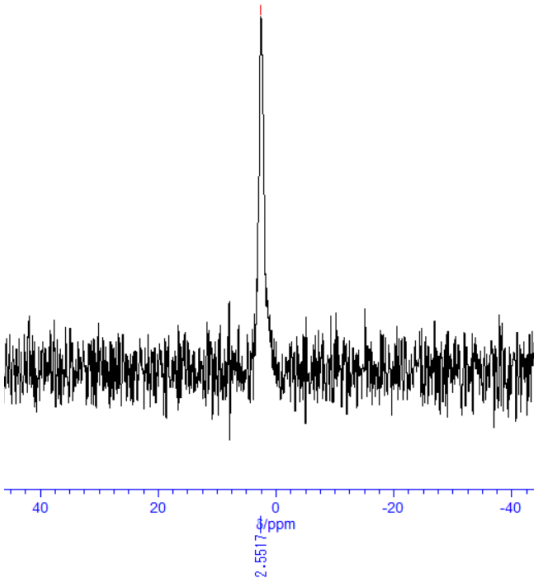

Chart 12. ^{11}B NMR spectrum of **6b**.

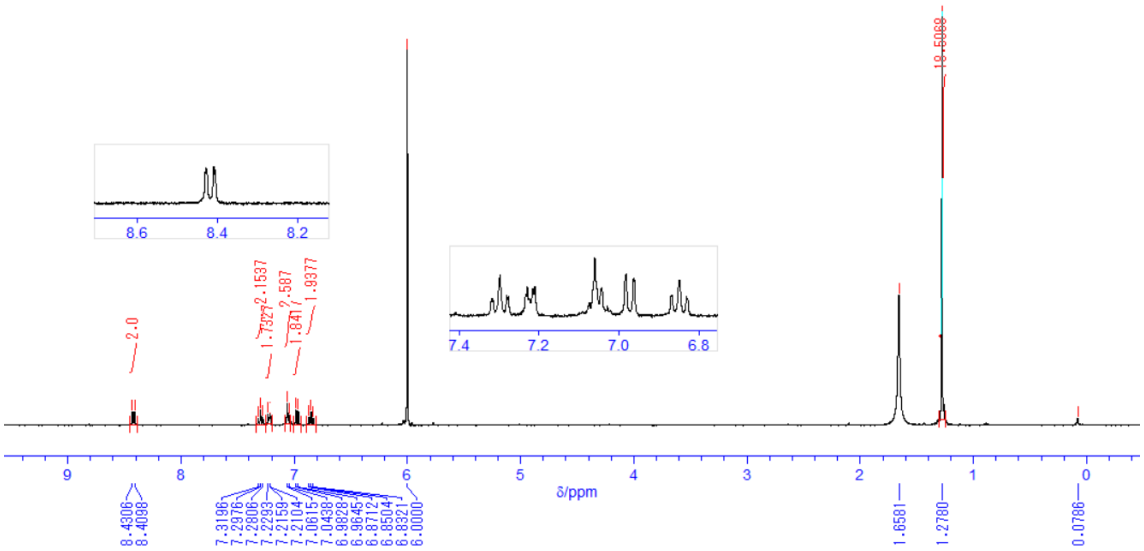

Chart 13. ^{1}H NMR spectrum of **6c**.

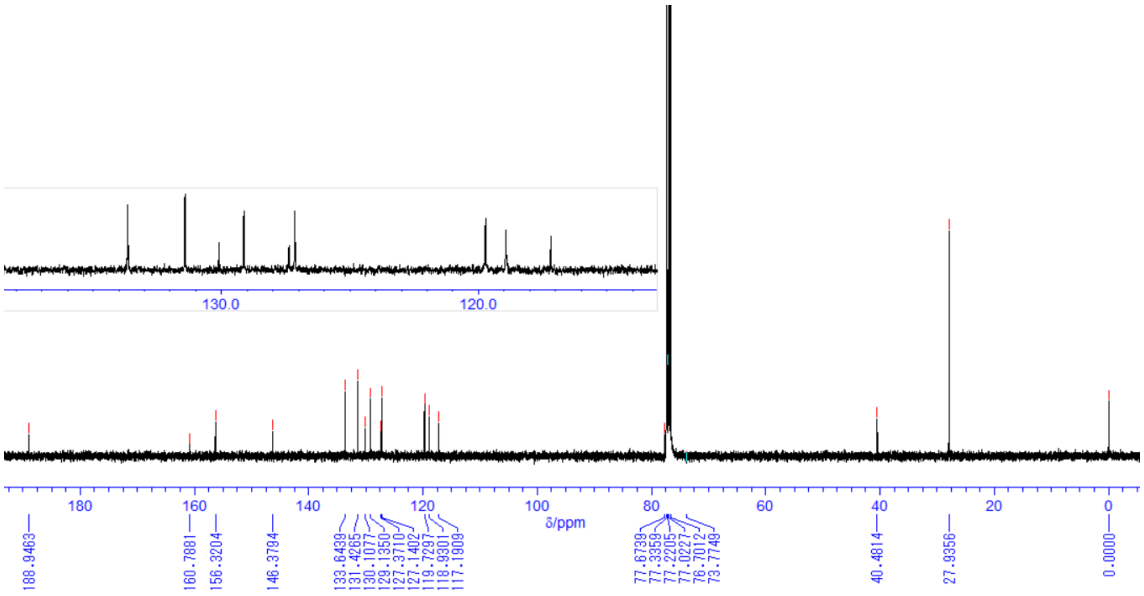

Chart 14. ^{13}C NMR spectrum of **6c**.

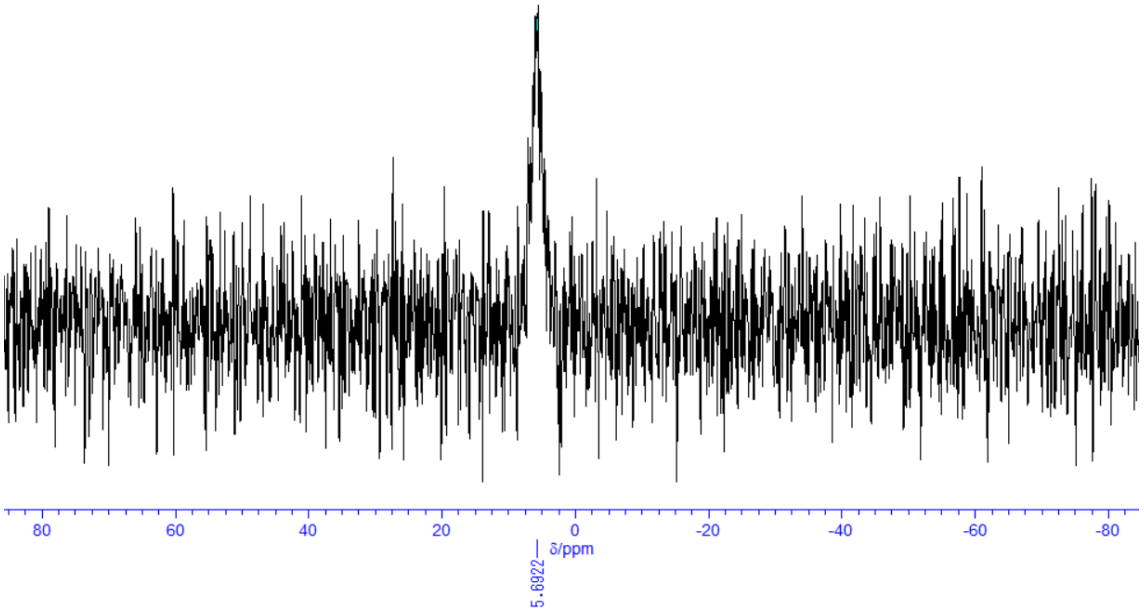

Chart 15. ^{11}B NMR spectrum of **6c**.

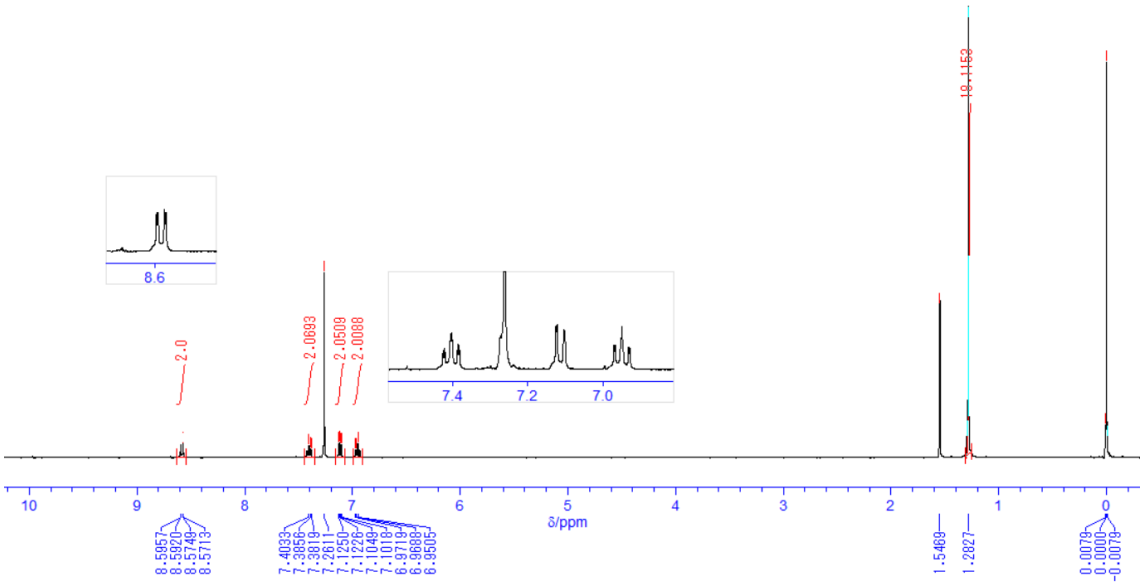

Chart 16. ^{1}H NMR spectrum of **6d**.

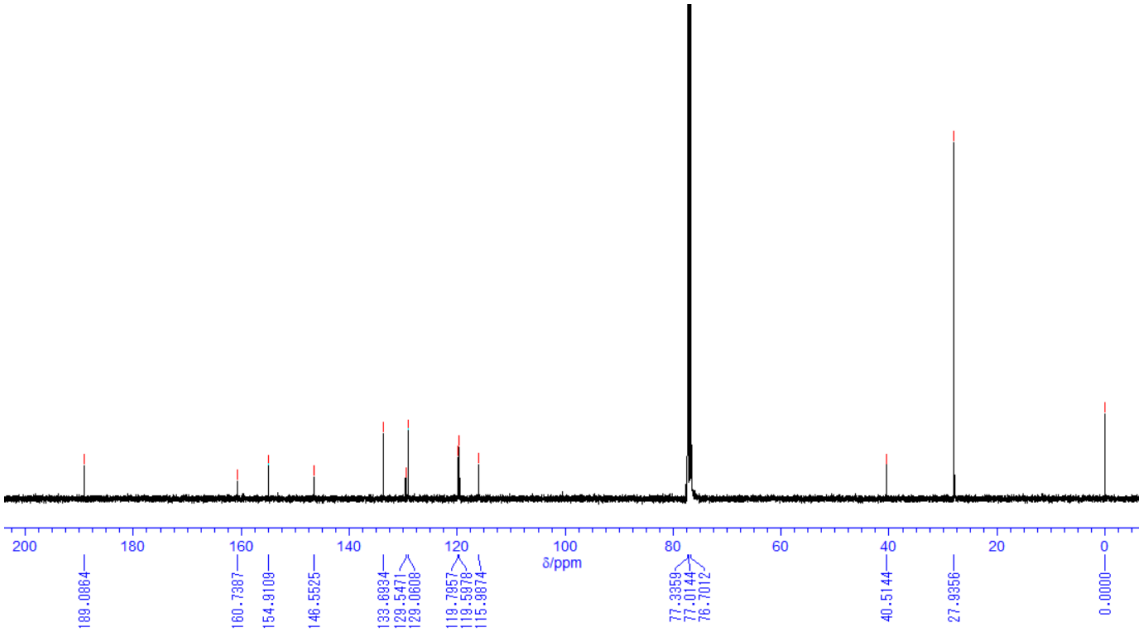

Chart 17. ^{13}C NMR spectrum of **6d**.

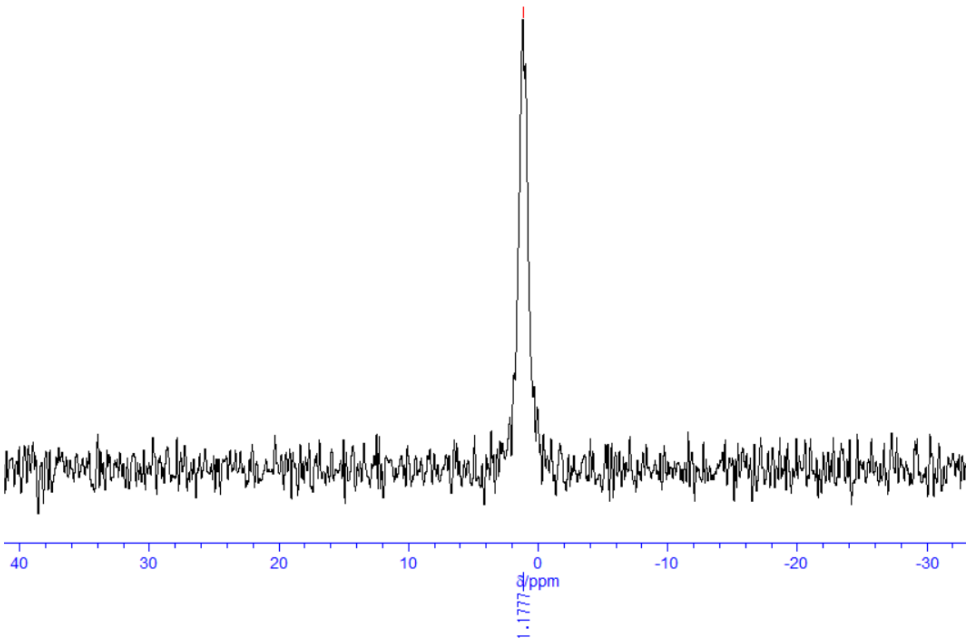

Chart 18. ^{11}B NMR spectrum of **6d**.